Velocity variability in a cross-section of a well-mixed estuary

by Björn Kjerfve[1] and Jeffrey A. Proehl[1]

ABSTRACT

North Inlet, South Carolina, is a well-mixed, tidally driven, high-salinity, shallow type 1A estuary consisting of winding creeks that intersect a 30 km² *Spartina alterniflora* salt marsh. An intensive spring tide field sampling in a 320 m wide cross-section during three consecutive tidal cycles in November 1977 resulted in detailed information on the cross-sectional net and root-mean-square (r.m.s.) velocity distributions. Although the estuary is well-mixed, both net and r.m.s. velocities vary significantly across the estuary, the deep channel typically experiencing net ebb flow and the secondary channel sometimes exhibiting net flood flow. Two high velocity cores reoccur in the same cross-sectional location each tidal cycle. Large variations in the net cross-section discharge occurred from cycle to cycle, apparently related to diurnal tide inequality. The results indicate that if material flux estimates are to be made in this type of estuary, the velocity is likely to be the parameter which requires the most dense sampling.

1. Introduction

With respect to circulation and dynamic structure, estuarine variations (particularly in velocity and salinity) are usually thought of as being two-dimensional, taking place along the longitudinal and vertical axes. It has been common practice to assume that lateral variations are comparatively small. In fact, the elegant and useful circulation-stratification classification method (Hansen and Rattray, 1966) ignores lateral gradients. Only in very large estuaries such as Chesapeake Bay (Pritchard, 1956) or Portland Inlet, British Columbia (Cameron, 1951), have lateral density gradients been shown to be approximately balanced by the Coriolis acceleration, i.e. conservation of momentum across the estuary is almost in a geostrophic equilibrium.

However, it is only recently that lateral gradients in partially or well-mixed estuaries have received focused attention. Fischer (1972), Dyer (1974, 1977, 1978), and Murray and Siripong (1978) demonstrated that with respect to longitudinal dispersion of salt and sediment, lateral variability plays as large a role as vertical gradients. Also, Dyer (1977) added to the Hansen-Rattray (1966) classification method by including lateral circulation and stratification effects. In spite of these

1. Belle W. Baruch Institute for Marine Biology and Coastal Research, Marine Science Program and Department of Geology, University of South Carolina, Columbia, South Carolina, 29208, U.S.A.

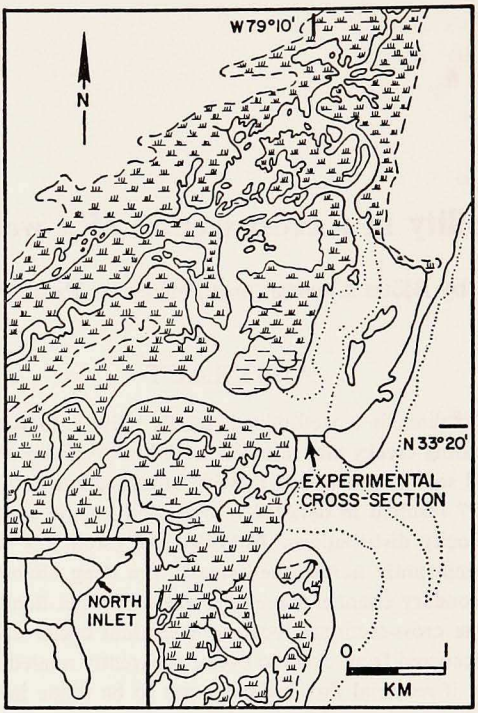

Figure 1. Area map of the North Inlet, South Carolina, estuary with the 320 m wide experimental cross-section indicated.

efforts, much work remains to be done before the three-dimensional structure of even the simplest of prototype estuaries is known and understood.

Pritchard (1955) pointed out that shallow, wide estuaries with low freshwater discharge and an appreciable tidal range are vertically homogeneous. Still, they may exhibit oppositely directed, time-averaged (net) currents across an estuary section. Such lateral net current shear exists consistently in the North Inlet estuary, South Carolina (Kjerfve, 1978).

The objective of this paper is to describe in detail how the longitudinal current velocity varies in a cross-section of the North Inlet estuary. This will illustrate the complex nature of the velocity structure in a well-mixed estuary. If material flux is the end product and a constituent concentration is almost uniform in the cross-section (as is often the case in well-mixed estuaries), a detailed knowledge of the velocity distribution normal to the cross-section is essential for flux computations. The quality of most flux estimates will thus largely depend on the degree to which the instantaneous velocity distribution is known.

2. Measurements and analysis

North Inlet, South Carolina (Fig. 1), is a 34 km^2 marsh-estuary situated just to

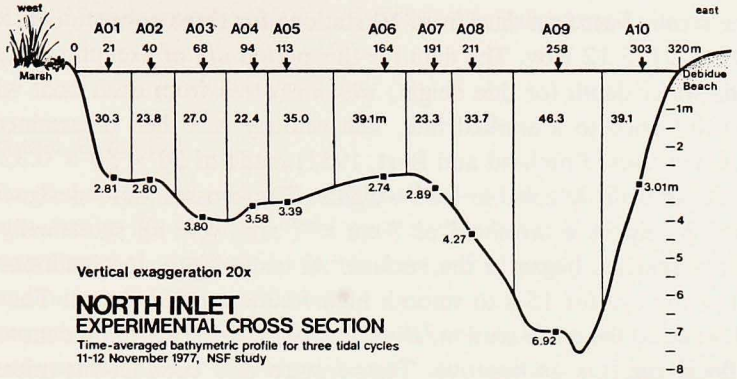

Figure 2. The experimental cross-section at mean tide showing 1) station notation (top row); 2) distance of station in meters from the western bank (second row); 3) distance in meters of each subsection over which measurements at a given station are considered representative (third row); and 4) time-averaged water depths (m) at each station (below the bottom trace).

the north of Winyah Bay. It consists of tidal creeks that wind sinuously through a *Spartina alterniflora* salt marsh. Most of the water exchange between the North Inlet system and the coastal ocean takes place through a barrier island inlet with only limited exchange through Winyah Bay. North Inlet is characterized by high salinities, 30-34 ppt; typical channel depths of 5 m; a semidiurnal tide; a neap tide range of 0.9 m and a maximum spring range of 2.5 m; maximum tidal currents less than 2.3 m s^{-1}; and negligible fresh water runoff.

As a part of a multi-disciplinary investigation of the total material flux between the North Inlet estuary and the coastal ocean, we measured velocity, temperature, and conductivity at 11 stations in a 320 m wide cross-section (Figs. 1, 2) over six tidal cycles 10-13 November 1977, coinciding with a new moon spring tide. Sampling occurred simultaneously at the 11 stations every 30 minutes on the hour and half-hour with measurements at meter intervals from surface to bottom. Each station consised of a 5 m long boat, which was four-point moored to diver-installed augers in the channel bottom. A total of 125 students/technicians/faculty helped with the field sampling. They were divided into three work shifts, which were rotated around the clock. A crew of 3-5 per boat made the measurements, including water samples and plankton and fish tows. Our study represents one of the most intensive synoptic field efforts ever in any estuary. The spatial measurements density may not be as great as in Boon's (1973) sediment flux study, but North Inlet's mean cross-sectional area of 1200 m^2 is almost 100 times larger than little Fool Creek, Virginia.

Because of adverse wind conditions at the beginning and end of the study, we suffered data loss and had one boat swamp and sink. For these reasons, we will only

present the results based on data from 10 stations for three consecutive tidal cycles, 0745 11 Nov.-2115 12 Nov. The data for this period are of exceptional quality.

First, the water depth (or tide height) was measured from each boat with a 5 kg lead weight attached to a marked line. The velocity was then determined with biplane current crosses (Pritchard and Burt, 1951) made of 20 × 50 × 0.32 cm stainless steel sheets with detachable lead weights. The crosses were designed to have ± 2 cm s^{-1} precision, a threshold of 7 cm s^{-1}, and were all statistically intercalibrated. Measurements began at the surface. At each depth, the inclinometer angle was averaged by eye for 15 s to smooth high frequency turbulence. The flow is at all times normal to the cross-section, allowing ebbing currents to be denoted as positive and flood currents as negative. Temperature and conductivity measurements were made with Beckman RS5-3 *in situ* induction salinometers and the salinity was computed (Kjerfve, in press). Temperature and salinity will not be discussed beyond the fact that the instantaneous values varied only slightly from the net cross-sectional means, 17.1°C and 33.0 ppt, respectively. The entire measurement cycle was repeated in the same order and completed in approximately 5 minutes.

Vertical profiles were computer fitted to the instantaneous velocity measurements, using a cubic spline algorithm with a logarithmic bottom boundary match (Kjerfve, in press). Equispaced, interpolated velocity values were used to compute net velocities at 11 depths from surface to bottom at the ten stations for each of the three tidal cycles (Kjerfve, 1975; in press). At the bottom the velocity was assumed to vanish. Similarly, we computed root-mean-square (r.m.s.) deviations from the 11 net values for each station and tidal cycle. The r.m.s. values are computed identically to the standard deviation, but there is no assumption that the population of velocity values is normally distributed. Each tidal cycle was taken to be 12.5 h long, thus consisting of 25 half-hourly measurement sets.

Also, instantaneous discharge, $Q(t)$, through the cross-section was calculated each half-hour from

$$Q(t) = \sum_{j=1}^{10} \{w_j h_j(t) \left[0.5\, v_{1j}(t) + \sum_{i=1}^{10} v_{ij}(t) \right] /10\}$$

(Kjerfve, in press, b) where i and j are depth and width counters, respectively; w is the width across the section for which the measurements from each station are assumed representative; $v(t)$ is time-varying velocity; and $h(t)$ is time-varying water depth. It should be noted that because the velocity vanishes at the bottom, $v_{11j}(t)$ does not appear in the above expression. Further, we assumed that each sub-section width, w_j, was constant with depth with a plane bottom at the measured depth, $h_j(t)$ (cf. Fig. 2). However, we did let elements w_1 and w_{10} increase with a linearly sloping embankment, beginning when the water level exceeded the time-averaged tide level. This would incorporate an estimate of the water discharge across the

marsh and sand beach west and east of the experimental transect, respectively, during high tides.

3. Results and discussion

Isopleths of net (Fig. 3) and r.m.s. (Fig. 4) velocities are shown for the experimental cross-section for the three tidal cycles. The isotachs reveal much about the velocity structure of the well-mixed North Inlet, which is a 1A estuary according to the Hansen-Rattray (1966) classification.

As indicated by the high mean salinity, 33.0 ppt, there was little fresh water (surface and ground water) input into North Inlet during the study. Still, the calculated net velocities were appreciable, reaching a spatial maximum of 48 cm s^{-1} in the ebb-direction in the deep channel for the third cycle. The maximum flood-directed net velocity was -21 cm s^{-1} on the western side of the cross-section for the second cycle. During tidal cycles one and three, the net velocity was everywhere ebb-directed with well-developed net current cores in the deep channel and in the vicinity of the secondary channel on the western side. During cycle two, on the other hand, the net current was directed oppositely on either side of the cross-section. The net ebb-core was still present in the deep channel, whereas the secondary channel now experienced net flood flow.

The net circulation in North Inlet is primarily driven by tidal pumping. Cross-sections typically exhibit bimodal bathymetry with one deep and one secondary channel. Kjerfve (1978) showed that the deep channel is ebb-dominant, usually corresponding to net ebb flow whereas the secondary channel commonly experiences net flood flow. This would classify North Inlet as a type C estuary (Pritchard, 1955) with respect to its circulation. There obviously exists a feedback between the circulation and the bimodal lateral bathymetry, probably related to overall creek geometry, channel curvature, and secondary currents (Kjerfve, 1978). The present data support this model of the North Inlet circulation but also indicate that the net cross-sectional velocity distribution varies greatly from one tidal cycle to another. The net discharge changed between the cycles from + 92 to − 118 to + 340 $m^3 s^{-1}$, respectively. The reasons for this will be discussed later.

Further the r.m.s. isotachs (Fig. 4) show that the highest velocities reoccur in the same location of the cross-section from cycle to cycle. The greatest velocity is persistently found in a near-surface core at station 2, just west of the secondary channel. The maximum r.m.s. value here reached 158 cm s^{-1}, which corresponds to a peak instantaneous current of 223 cm s^{-1} (= r.m.s. value $\times \sqrt{2}$), assuming a sinusoidal velocity change over the tidal cycle. In comparison, the maximum *measured* current was 232 cm s^{-1}. A second ebb and flood velocity core existed in the deep channel. It was especially pronounced close to the bottom during the third tidal cycle, when the maximum r.m.s. value was 130 cm s^{-1}.

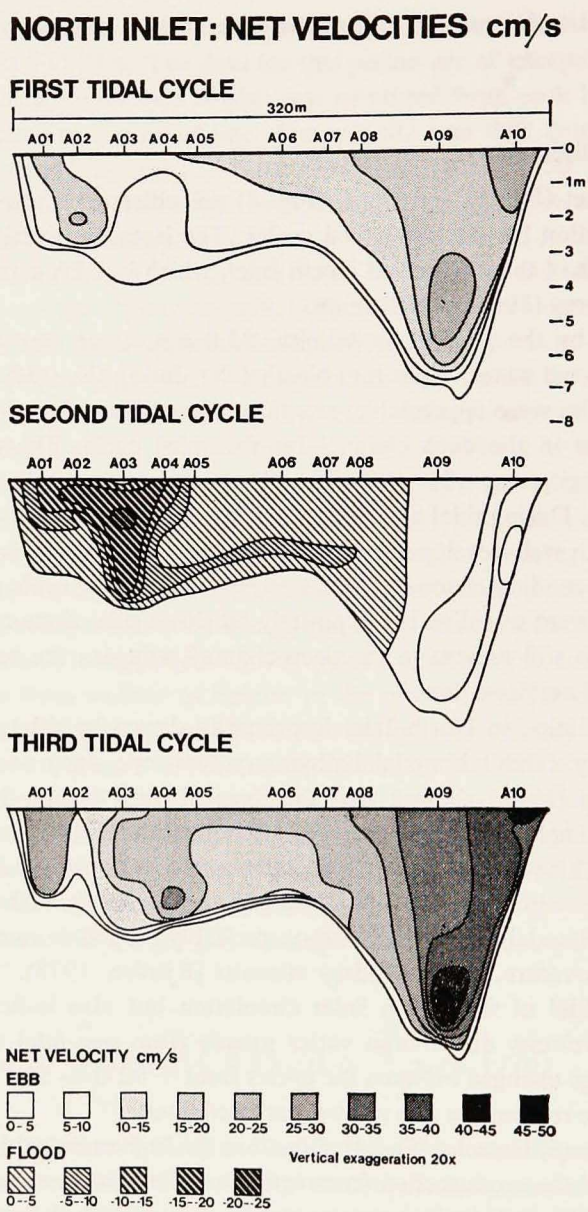

Figure 3. Isopleths of net longitudinal velocities (cm s^{-1}) in the experimental cross-section for each of the three tidal cycles.

There are several possible reasons for this distribution of the r.m.s. velocity. However, we can at best guess that the cross-sectional distribution of the peak currents somehow relates to 1) channel curvature; 2) the existence of an extensive flood-tidal delta oceanward of the experimental cross-section; 3) lateral bathymetry; and 4) the

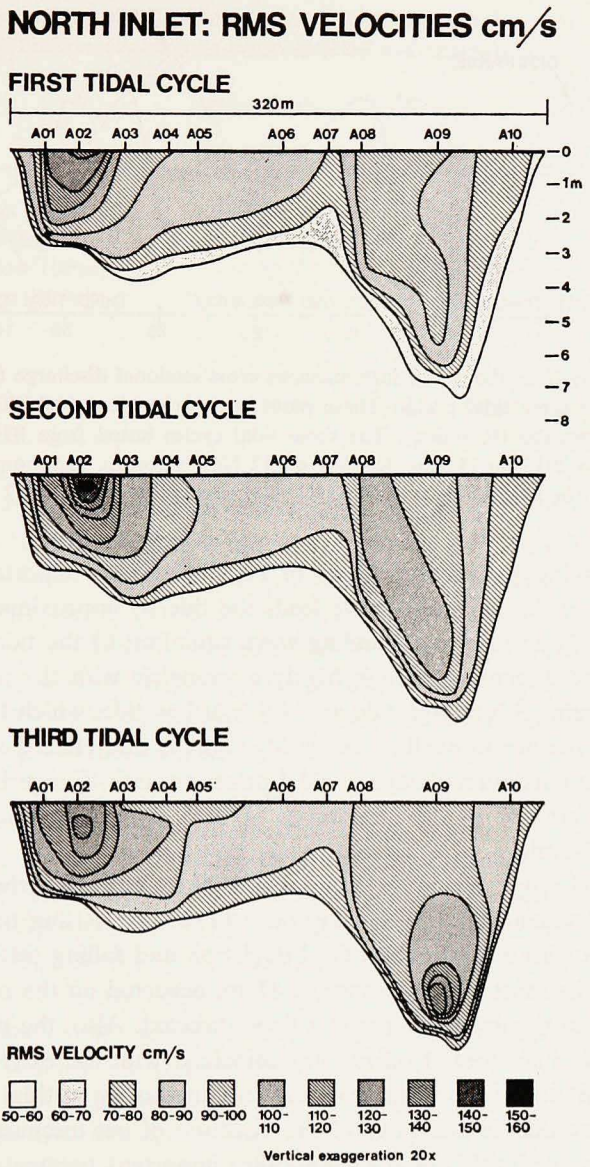

Figure 4. Isopleths of root mean squared deviations (cm s^{-1}) from the net velocities shown in Figure 1 for each of the three tidal cycles.

junction of two tidal creeks just landward of the cross-section. To include this kind of cross-sectional velocity variability in any kind of modelling would be a complex undertaking. Still, in the computation of material flux, it should be obvious that the velocity cannot be taken to be constant in the cross-section, a common assumption.

The instantaneous cross-sectional discharge and water level variations for this

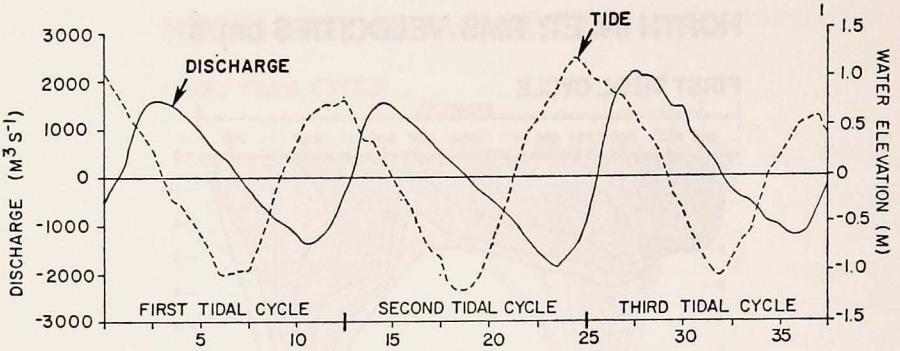

Figure 5. Time-variations (hours) of instantaneous cross-sectional discharge ($m^3\ s^{-1}$) and water level (m) for the three tidal cycles. These plots incorporate every velocity and water level measurement from the 10 stations. The three tidal cycles lasted from 0745 to 2015 on 11 Nov. (first), from 2015 on 11 Nov. to 0845 on 12 Nov. (second), and from 0845 to 2115 on 12 Nov. (third). The plot begins at 0800 on 11 Nov. and ends at 2100 on 12 Nov.

spring tide sampling period are shown in Fig. 5. Several important features are readily noticed: a) the discharge curve leads the tide by approximately $\pi/2$ rad as can be expected in an idealized standing wave situation; b) the tidal curve is quite symmetric; c) the discharge curve is highly asymmetric with the time-lag between the two curves being 3 h at high tide and 4.5 h at low tide, which Boon (1975) explained by the presence of shallow water M_4 and M_6 tide effects, and which is intuitively due to a maximum change in tidal prism per unit change in tidal elevation around high water; and d) the amplitudes of both curves vary significantly from half-cycle to half-cycle.

The mean tidal range during the study was 2.03 m. However, the variability was considerable, particularly between rising tides (Table 1). Rising tides had a mean range of 1.95 m with a 0.40 m standard deviation and falling tides had a 2.10 ± 0.15 m range. The most extreme range, 2.41 m, occurred on the rising tide on the second cycle when the net discharge was flood directed. Also, the rising tide during the third cycle was smallest, 1.62 m, and coincided with the extreme net ebb discharge of 340 $m^3\ s^{-1}$. Thus, it appears that the inequality in tidal ranges, particularly on the rising tide, is indicative of the direction of net discharge from cycle to cycle. The net water level is obviously another important parameter related to the net discharge and discharge direction, although this particular record is too short to low-pass-filter.

Overall, the net discharge was ebb-directed, 105 $m^3\ s^{-1}$ with a r.m.s. deviation of 1,114 $m^3\ s^{-1}$, and a peak discharge of 2,135 $m^3\ s^{-1}$ on the ebbing portion of the third cycle (Table 1). The variability is obviously too great for any reliability to be placed on the overall mean as an indicator of the long-term discharge rate. It does, however, point to the need for long-term sampling (cf. Weisberg, 1976). In the ab-

Table 1. Comparison of rising and falling tidal range and ebb and flood discharge rates for the three tidal cycles. Positive discharge is ocean directed and negative discharge is directed into the estuary.

	Tidal Cycle 1	Tidal Cycle 2	Tidal Cycle 3
Rising range (m)	1.81	2.41	1.64
Falling range (m)	2.05	1.99	2.27
Max. flood discharge (m^3/s)	−1,392	−1,888	−1,218
Max. ebb discharge (m^3/s)	1,599	1,571	2,135
Cumulative flood flow ($10^6 m^3$)	−17.97	−24.84	−15.19
Cumulative ebb flow ($10^6 m^3$)	22.11	19.53	30.47
Net discharge (m^3/s)	92	−118	340

sence of substantial amounts of freshwater runoff, the drastic variation in net discharge rates implies that a portion of the tidal prism is either flushed from (+ flow) or stored in (− flow) the estuary from cycle to cycle. For these three tidal cycles, the mean falling range exceeded the mean rising range by 0.2 m and at the same time the system exported water at a net rate of 105 $m^3\ s^{-1}$. Thus net transports of water and most likely also dissolved/suspended materials are at least partially caused by variations in tide range due to astronomical forcing (diurnal inequality) or local wind effects. However, given a longer time record, it is likely that far-field forcing from the coastal ocean (Wang and Elliott, 1978; Kjerfve *et al.*, 1978) can also be shown to cause low-frequency variations in the net discharge rate and direction, associated with continental shelf waves and upwelling events.

4. Summary

The North Inlet estuary is classified as a well-mixed estuary but exhibits significant variations in the net and r.m.s. isotachs in an experimental cross-section and shows variations from tidal cycle to tidal cycle. An intensive field project, sampling 10 stations in a 320 m cross-section every half-hour for three tidal cycles with 125 field workers, allows us to draw the following conclusions:

1. The deep channel experiences net ebb flow, whereas the secondary channel in the cross-section is more susceptible to net flood flow.
2. There exist two high-velocity cores, as indicated by the r.m.s. isotachs, which reoccur in the same location during each tidal cycle.
3. Drastic net discharge variations may occur between tidal cycles because of differences in tidal range or far-field forcing—this points to the necessity for long-term measurements to establish reliability in the overall net values.
4. In making mass flux calculations of a suspended or dissolved constituent, particular attention must be paid to the highly variable velocity although the constituent concentration may be almost homogeneous in the cross-section.
5. The velocity structure of even a well-mixed estuary is highly complex and should not be modelled with an area-averaged velocity-mean.

Acknowledgments. We thank the 125 faculty, technicians, and students from the University of South Carolina Marine Science Program, who diligently collected the field data. We are especially grateful to S. E. Stancyk, J. E. Greer, Linda D'Apolito and F. B. Schwing. Janet Drasites and Lucy Kjerfve did the drafting. This project was supported by National Science Foundation Grant No. DEP76-83010. This paper is Contribution No. 273 from the Belle W. Baruch Institute for Marine Biology and Coastal Research.

REFERENCES

Boon, J. D., III. 1973. Sediment transport processes in a salt marsh drainage system. Ph.D. Thesis, College of William and Mary, Williamsburg, Va., 226 pp.

—— 1975. Tidal discharge asymmetry in a salt marsh drainage system. Limnol. Oceanogr., *20,* 71–80.

Cameron, W. M. 1951. On the transverse forces in a British Columbia inlet. Trans. Royal Soc. Canada, *45,* Series III, 1–8.

Dyer, K. R. 1974. The salt balance in stratified estuaries. Estuarine and Coastal Mar. Sci., *2,* 273–281.

—— 1977. Lateral circulation effects in estuaries, *in* Estuaries, Geophysics and the Environment, C. B. Officer, ed., National Academy of Sciences, Washington, D.C., 127 pp.

—— 1978. The balance of suspended sediment in the Gironde Thames Estuaries, *in* Estuarine Transport Processes, B. Kjerfve, ed., Univ. South Carolina Press, Columbia, 331 pp.

Fischer, H. B. 1972. Mass transport mechanisms in partially stratified estuaries. J. Fluid Mechanics, *53,* 671–687.

Hansen, D. V., and M. Rattray, Jr. 1966. New dimensions in estuary classification. Limnol. Oceanogr., *11,* 319–326.

Kjerfve, B. 1975. Velocity averaging in estuaries characterized by a large tidal range to depth ratio. Estuarine and Coastal Mar. Sci., *3,* 311–323.

—— 1978. Bathymetry as an indicator of net circulation in well-mixed estuaries. Limnol. Oceanogr., *23,* 816–821.

—— In press. Measurement and analysis of water current, temperature, salinity, and density, *in* Hydrography and Sedimentation in Estuaries, K. R. Dyer, ed. Cambridge Univ. Press, Cambridge, U.K.

Kjerfve, B., J. E. Greer, and R. L. Crout. 1978. Low-frequency response of estuarine sea level to non-local forcing, *in* Estuarine Interactions, M. L. Wiley, ed. Academic Press, New York, 603 pp.

Murray, S. P. and A. Siripong. 1978. Role of lateral gradients and longitudinal dispersion in the salt balance of a shallow, well-mixed estuary, *in* Estuarine Transport Processes, B. Kjerfve, ed., Univ. South Carolina Press, Columbia, 331 pp.

Pritchard, D. W. 1955. Estuarine circulation patterns. Proc. Am. Soc. Civil Eng., *81,* 717/1–717/11.

—— 1956. The dynamic structure of a coastal plain estuary. J. Mar. Res., *15,* 33–42.

Pritchard, D. W., and W. V. Burt. 1951. An inexpensive and rapid technique for obtaining current profiles in estuarine waters. J. Mar. Res., *10,* 180–189.

Wang, D. P., and A. J. Elliott. 1978. Non-tidal variability in the Chesapeake Bay and Potomac River: evidence for non-local forcing. J. Phys. Oceanogr., *8,* 225–232.

Weisberg, R. H. 1976. A note on estuarine mean flow estimation. J. Mar. Res., *34,* 387–394.

Received: *14 August, 1978;* revised: *26 March, 1978.*